NASA/TM-20210018094

Proton Exchange Membrane Fuel Cell Transient Load Response

Phillip J. Smith, William R. Bennett, Ian J. Jakupca, and Ryan P. Gilligan
Glenn Research Center, Cleveland, Ohio

Lawrence G. Edwards
Vantage Partners, LLC, Brook Park, Ohio

December 2021

NASA STI Program . . . in Profile

Since its founding, NASA has been dedicated to the advancement of aeronautics and space science. The NASA Scientific and Technical Information (STI) Program plays a key part in helping NASA maintain this important role.

The NASA STI Program operates under the auspices of the Agency Chief Information Officer. It collects, organizes, provides for archiving, and disseminates NASA's STI. The NASA STI Program provides access to the NASA Technical Report Server—Registered (NTRS Reg) and NASA Technical Report Server—Public (NTRS) thus providing one of the largest collections of aeronautical and space science STI in the world. Results are published in both non-NASA channels and by NASA in the NASA STI Report Series, which includes the following report types:

- TECHNICAL PUBLICATION. Reports of completed research or a major significant phase of research that present the results of NASA programs and include extensive data or theoretical analysis. Includes compilations of significant scientific and technical data and information deemed to be of continuing reference value. NASA counter-part of peer-reviewed formal professional papers, but has less stringent limitations on manuscript length and extent of graphic presentations.

- TECHNICAL MEMORANDUM. Scientific and technical findings that are preliminary or of specialized interest, e.g., "quick-release" reports, working papers, and bibliographies that contain minimal annotation. Does not contain extensive analysis.

- CONTRACTOR REPORT. Scientific and technical findings by NASA-sponsored contractors and grantees.

- CONFERENCE PUBLICATION. Collected papers from scientific and technical conferences, symposia, seminars, or other meetings sponsored or co-sponsored by NASA.

- SPECIAL PUBLICATION. Scientific, technical, or historical information from NASA programs, projects, and missions, often concerned with subjects having substantial public interest.

- TECHNICAL TRANSLATION. English-language translations of foreign scientific and technical material pertinent to NASA's mission.

For more information about the NASA STI program, see the following:

- Access the NASA STI program home page at http://www.sti.nasa.gov

- E-mail your question to help@sti.nasa.gov

- Fax your question to the NASA STI Information Desk at 757-864-6500

- Telephone the NASA STI Information Desk at 757-864-9658

- Write to:
  NASA STI Program
  Mail Stop 148
  NASA Langley Research Center
  Hampton, VA 23681-2199

NASA/TM-20210018094

Proton Exchange Membrane Fuel Cell Transient Load Response

Phillip J. Smith, William R. Bennett, Ian J. Jakupca, and Ryan P. Gilligan
Glenn Research Center, Cleveland, Ohio

Lawrence G. Edwards
Vantage Partners, LLC, Brook Park, Ohio

National Aeronautics and
Space Administration

Glenn Research Center
Cleveland, Ohio 44135

December 2021

Level of Review: This material has been technically reviewed by technical management.

Available from

NASA STI Program
Mail Stop 148
NASA Langley Research Center
Hampton, VA 23681-2199

National Technical Information Service
5285 Port Royal Road
Springfield, VA 22161
703-605-6000

This report is available in electronic form at http://www.sti.nasa.gov/ and http://ntrs.nasa.gov/

Proton Exchange Membrane Fuel Cell Transient Load Response

Phillip J. Smith, William R. Bennett, Ian J. Jakupca, and Ryan P. Gilligan
National Aeronautics and Space Administration
Glenn Research Center
Cleveland, Ohio 44135

Lawrence G. Edwards
Vantage Partners, LLC
Brook Park, Ohio 44142

Summary

Spaceflight mission profiles may not be limited to constant power loads. It is necessary for the associated power system to support changes in load in addition to being energy dense. H_2-O_2 proton exchange membrane (PEM) fuel cells can accommodate such requirements without significant current smoothing or additional devices to provide transient power. This testing involved current load step changes to characterize non-flow-through PEM fuel cell response to increasing and decreasing load step changes over a range of 0 to 0.5 A/cm^2. It was determined that fuel cell output voltage stabilizes within 4 ms with no noticeable steady-state performance degradation, following exposure of the fuel cell to transient loads of up to ~1.5 A/cm^2. Faster stabilization generally occurred following larger step changes.

Nomenclature

A	active area
C	capacitance
E	current sensor voltage output
i	current density
GDL	gas diffusion layer
NFT	non-flow-through
PEM	proton exchange membrane
R	resistance
x	current sensor output scaling factor

Introduction

Many spaceflight missions require power sources capable of supporting rapid and significant load changes in addition to long-term steady-state operation. Not every power system is capable of meeting both requirements, but it is expected that proton exchange membrane (PEM) fuel cells can support all types of load without the need for current smoothing. NASA has long employed a standardized fuel cell test load profile based on actual space shuttle flight data used for ongoing fuel cell development activities. This 2-h load profile, preceded and followed by current sweeps, is shown in Figure 1. The shortest pulse durations are 30 s to comply with NASA Handbook 8739.19-3, "NASA Measurement Quality Assurance Handbook," since the fuel cell test station is limited to a 1-Hz data capture rate. The maximum current load ratio is up to 8:1 in a single step change. Larger steps are expected in future NASA mission load profiles.

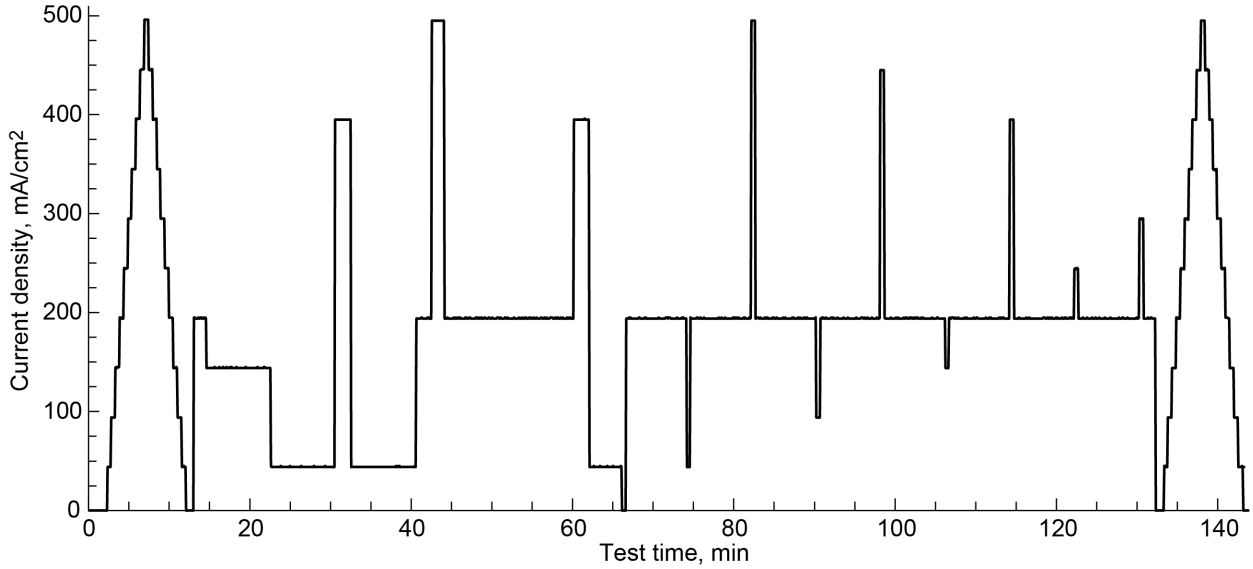

Figure 1.—Fuel cell load profile typically used for testing.

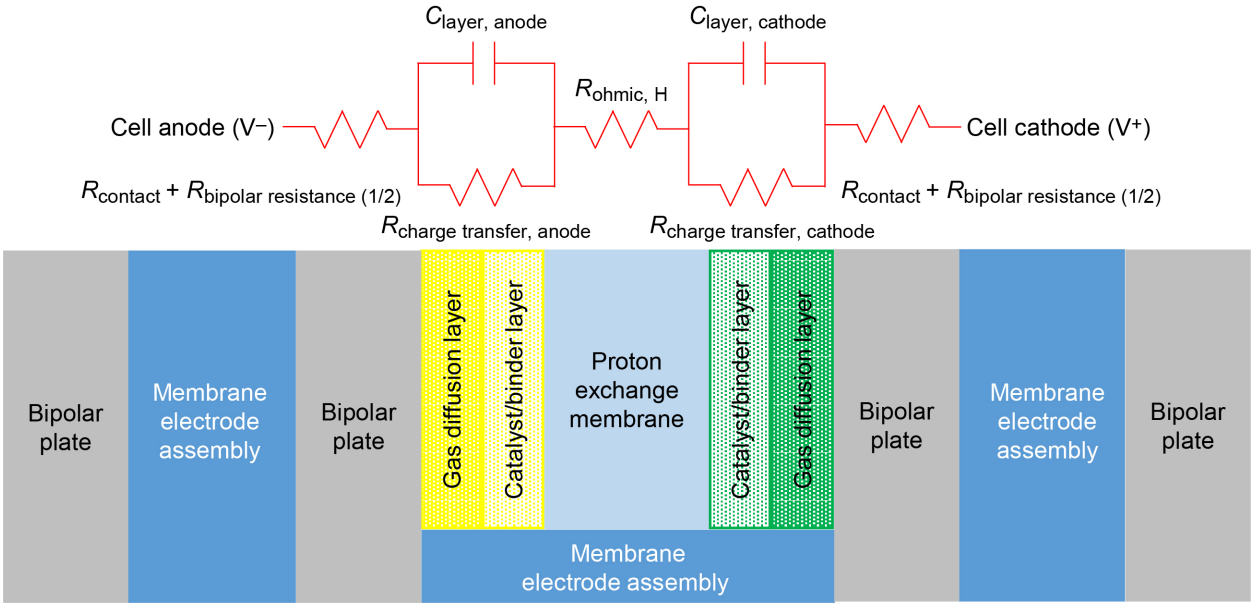

Figure 2.—Fuel cell physical construction related to representative equivalent circuit; *R* is resistance and *C* is capacitance.

In typical fuel cell tests, cell performance appears repeatable and stable under steady-state conditions. Even gradual load changes result in voltage response that directly follows the steady-state polarization curve. Maximum current and voltage rates of change (slew rates) are specific to the fuel cell stack and test hardware, and response times range from <5 to ~100 ms. The response characteristics are dependent on cell and stack construction, materials, and membrane electrode assembly double-layer capacitance. An equivalent electrical circuit is presented in Figure 2 and aligned with the relevant stack components. Although bipolar plates and PEMs are represented by pure resistors, there is a capacitive effect presented by the catalyst material and gas diffusion layer (GDL) combination adjacent to the PEM. This effect, in parallel with charge transfer resistance, provides the effective time constant for fuel cell response. After a step change in current, the system does not immediately return to steady-state conditions, and current-voltage

overshoot or undershoot is expected (Ref. 1). It is desired to empirically quantify this response for state-of-the-art aerospace PEM fuel cells.

This study was completed to evaluate fuel cell performance over the millisecond timescale prior to reaching steady-state operation. The test objective is to characterize the fuel cell stack response to step changes in an applied load. In a flight mission, a stack must supply power to hardware with variable demand characteristics (e.g. actuator in-rush current). This testing should provide necessary engineering data for target vehicle electrical system designers.

Experimental

A H_2-O_2 passive water removal non-flow-through (NFT) proton exchange membrane (PEM) fuel cell stack was utilized for this testing. This stack consisted of 12 cells with 50 cm^2 active area and is shown in Figure 3. It was developed and tested for a long-life regenerative fuel cell energy storage application and refurbished following a 2012 demonstration. Previous testing of this stack build at NASA consisted of supporting a load for 90.4 and 124.9 h of total testing, 18 2-h load profiles, 40 polarization curves, 26 start-up and shutdown cycles, and operation in three orientations with respect to gravity. The stack was exposed to launch vibration sensitivity testing while in a pressurized, but inert, non-operational state in a variety of stack orientations with respect to gravity (i.e., operational positions). No significant performance changes were found as a result of those evaluations (Ref. 2). The stack was also used for a reactant impurity sensitivity study and operation at reduced pressures (Refs. 3 and 4). The stack proved capable of operating with up to 30 percent helium in the reactant supply with flow-through reactants.

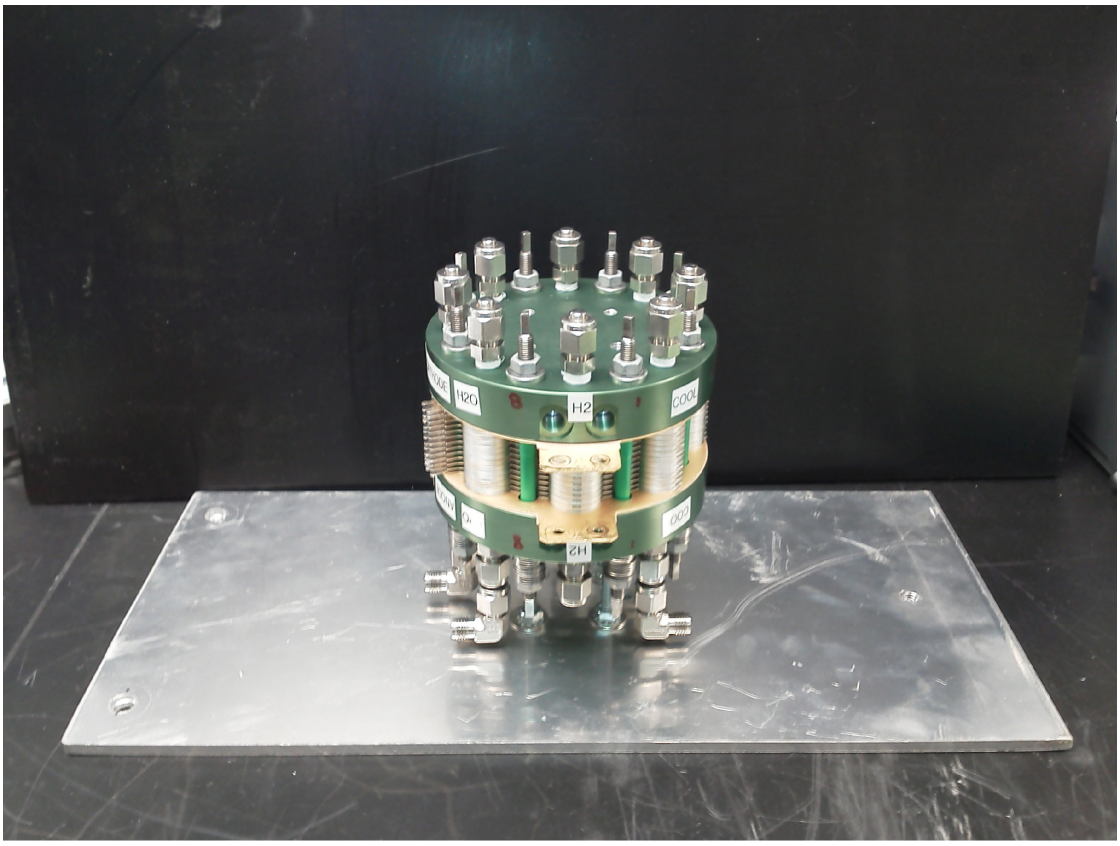

Figure 3.—Twelve-cell proton exchange membrane (PEM) fuel cell stack.

Starting from a steady-state condition and supplied with research-grade reactants, the testing consists of initiating the nominal current load changes shown in Table I on the fuel cell stack at the maximum slew rate of the selected electronic load (100 μs/ΔV). Voltage and current responses are monitored by an oscilloscope, placed between the fuel cell and the electronic load as shown in Figure 4, with data recorded over the selected time base at a sampling interval of 0.8 μs. That timescale allows for observation of rapid transient responses during step changes that are not captured by the existing data acquisition rate typically used for 2-h load profiles. The current facility is configured to characterize the fuel cell stack in isolation; the resistive electronic load and short leads do not simulate the impact of inductive or capacitive elements of a larger integrated system.

Data Analysis

The current sensor measurement is related to stack current density i (A/cm^2) by

$$i = \frac{E}{xA} \tag{1}$$

where E is the voltage output from the current sensor, x is the scaling factor equal to 0.012 V/A, and A is the stack active area per cell in square centimeters. For determination of test times to maximum current, minimum voltage, and current and voltage values at 90 and 99 percent of the change from initial to final conditions, the current density was smoothed by averaging values over ±2.4 μs.

TABLE I.—CURRENT DENSITY STEP CHANGES PERFORMED DURING TESTING

Case	Step increases, A/cm^2	Step decreases, A/cm^2
1	0 to 0.5	0.5 to 0
2	0 to 0.4	0.4 to 0
3	0 to 0.3	0.3 to 0
4	0 to 0.2	0.2 to 0

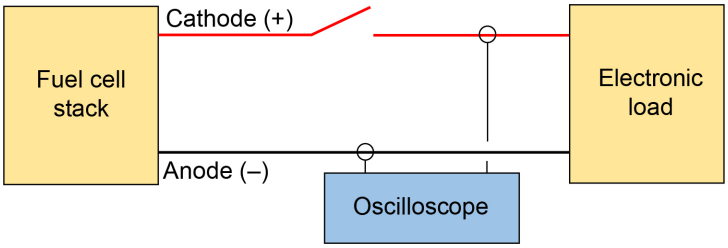

Figure 4.—Arrangement of fuel cell stack, oscilloscope, and electronic load during testing.

Results and Discussion

Step Increase

Figure 5 shows the average cell potential and current density results for the current load step increases. Raw data for all test cases are provided in the appendix.

Table II details the minimum individual cell potentials across the entire stack, maximum current density loads and powers produced, and the final average cell potentials 30 s after the load change command. Comparing the maximum current densities to the final nominal current density setpoint, it is likely that the high load overshoot observed in this step response test has occurred for all load step changes during testing at NASA using the same load control system. It suggests that a fuel cell stack will remain within the voltage window during transient loads.

One previous study noted more current overshoot with higher initial cell voltage, attributable to oxygen mass transfer issues (Ref. 5). Unfortunately, there is no applicable comparison in the set of cases presented here since all increasing current load changes began at the same open-circuit condition. When comparing steps that have a common initial voltage, response-time potential dependence may be most impacted when the final cell voltages were greater than 0.75 V and activation losses predominate (Ref. 6). The fact that the rate-limiting process was potential dependent suggests that it is related to charge transfer. Considering that the cathode was supplied with pure oxygen, it is possible that fuel cell response can be constrained by charge transfer (Ref. 6).

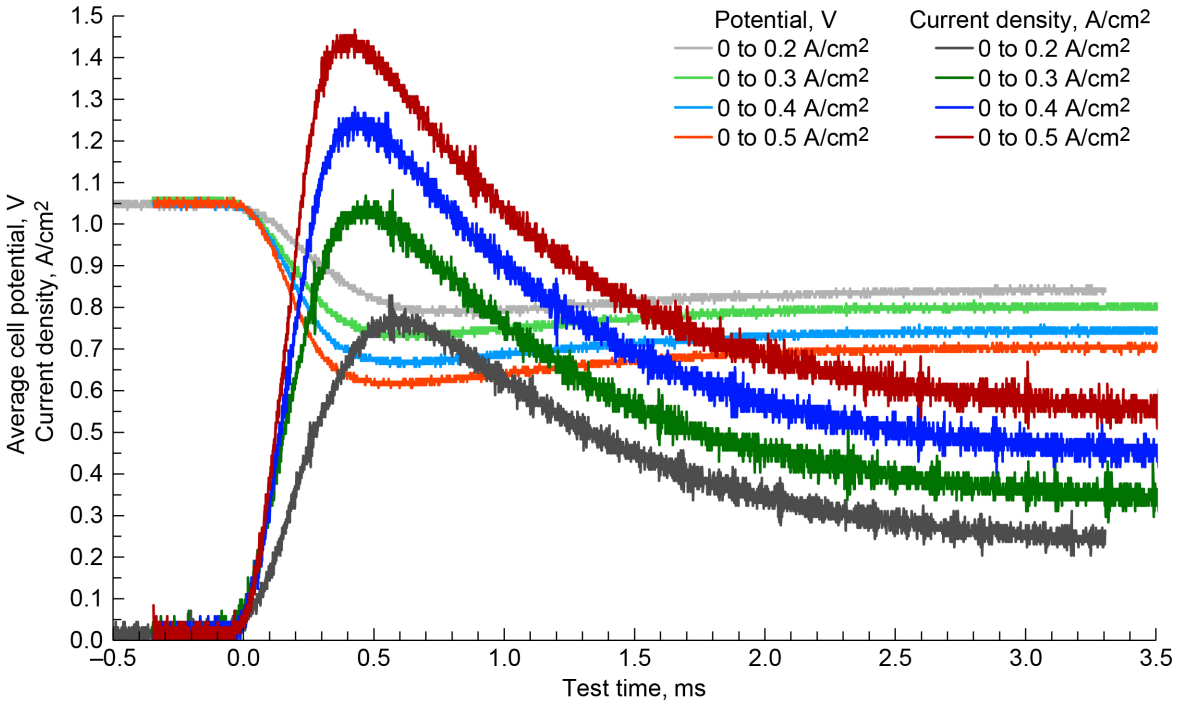

Figure 5.—Average fuel cell potential and current density for current load step increases where test time 0 ms indicates the load change command.

TABLE II.—NOTABLE FUEL CELL STACK PERFORMANCE METRICS FOR CURRENT LOAD STEP INCREASE CASES

Case, A/cm^2	Minimum cell potential, V	Maximum current density, A/cm^2	Maximum power, W/cm^2	Final cell potential,[a] V
0 to 0.5	0.60	1.467	0.958	0.707
0 to 0.4	0.65	1.280	0.884	0.742
0 to 0.3	0.72	1.080	0.799	0.797
0 to 0.2	0.77	0.827	0.667	0.835

[a]Potential measured at test time 30 s.

Other experimental studies indicated more voltage undershoot and longer time to steady state can result from inadequate reactant supply, lower temperature, greater current load change, poorer reactant humidification (with cathode-side humidification being more impactful, as anode-side humidification is naturally amended by water back-diffusion), and ineffective water removal (Refs. 6 to 8). The only identified processes that contribute to transient response over timescales relevant to PEM NFT response (milliseconds) are charging of the electric double layer (0.2 μs) and GDL diffusion. All other factors (e.g., water diffusion and accumulation, thermal changes, etc.) occur over longer timescales (Refs. 1 and 8).

Figure 6 shows the times to reach the minimum average cell voltage and maximum current density. It took ~0.4 to ~0.6 ms to reach maximum current, and minimum voltage lagged about ~0.2 ms behind. Greater current density step increases took less time to reach the voltage and current extremes compared to smaller current steps. Still, it is difficult to fully separate electrochemical physics for the various equivalent circuit elements of a fuel cell stack from the characteristics of the electronic load for these large direct currents. At longer time intervals, gas diffusion effects can look like capacitance charging (e.g., Warburg impedance) and present errors in double-layer capacitance measurement. Given the set slew rate of the electronic load for this 12-cell stack, a change from average cell voltage of 1.05 to 0.7 V should take ~0.4 ms, which accounts for the majority of the time to minimum voltage for each case in Figure 6. This indicates that the load is mostly driving the response. Alternating current impedance spectroscopy would help resolve the causation but was not incorporated in this work. A preferred experimental set up could be to use parallel path resistive circuits to enable rapid switching. This has been shown to enable switching in 3 μs and eliminate electronic load slew rate effects (Ref. 9).

It is common for studies on flow-through or H_2-air fuel cells to establish conditions where stacks are supplied inadequate reactants to support an increasing current load. In a past effort that incorporated sufficient time resolution on data collection and provided excess reactant gas, a fuel cell simply responded as quickly as the electronic load (Ref. 5). Voltage undershoot behavior was observed in a 330-cm^2 stack when changing current density from 0.303 to 1.00 A/cm^2 (Ref. 7). In this stack it took 1 s to reach the voltage minimum, the time to accommodate the gas convection and diffusion processes, and tens of seconds to obtain steady state when increasing load. Utilizing higher pressure pure reactants (i.e., oxygen rather than atmospheric pressure air) is expected to greatly shorten the response time. This is one factor in producing the millisecond response times reported in this work.

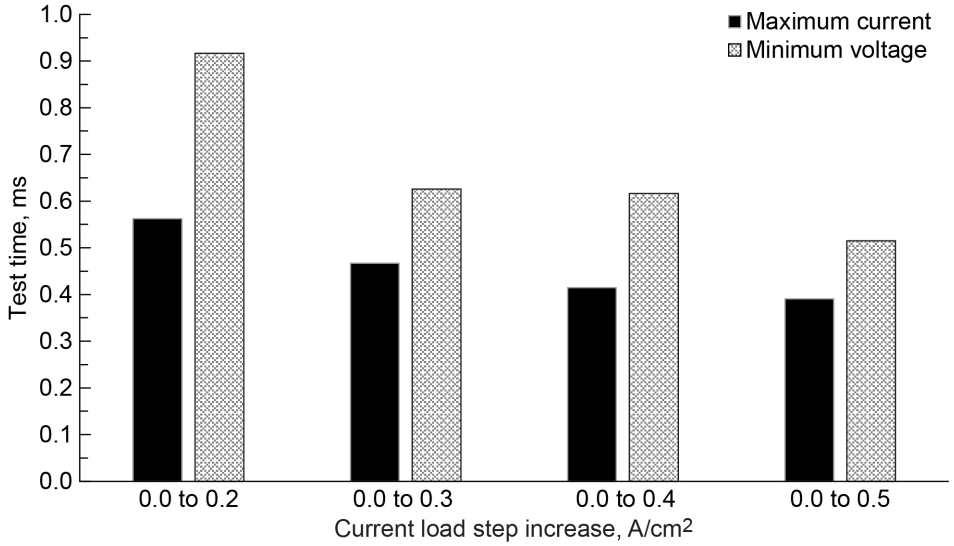

Figure 6.—Times to maximum current load and minimum average fuel cell voltage following current load step increases.

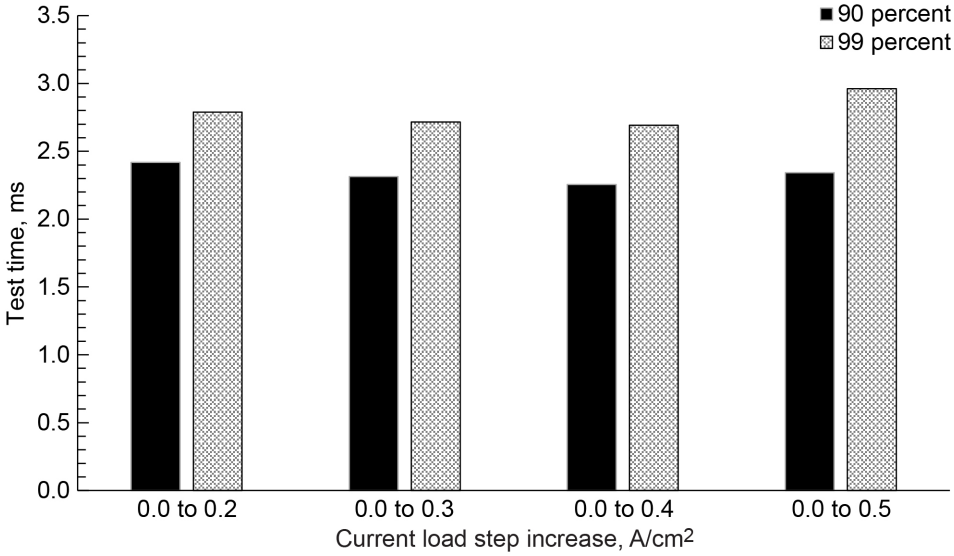

Figure 7.—Times to fuel cell current load at 90 and 99 percent of final change following current load step increases.

Figure 7 shows the times for current load to reach 90 and 99 percent of the final current density change, comparing the final steady-state current density and initial current density for the cases of current load step increase. Figure 8 displays the times for average cell voltage to reach within 90 and 99 percent of the final voltage change between initial and final steady-state values. Similar to the minimum voltage and maximum current trends, larger current steps generally resulted in shorter times to approach the final steady-state voltages and currents. The exceptions were all in the 0 to 0.5 A/cm^2 case, which suggests that this result could be a slight anomaly due to the single attempt for this (and each) case. One previous study performed each test case four times to enable averaged results (Ref. 9). Fuel cell results presented here are from cases that were only completed once, and this potentially contributed to trend inconsistencies. The 0 to 0.5 A/cm^2 case results could also be due to inaccurate determination or control of the end steady state.

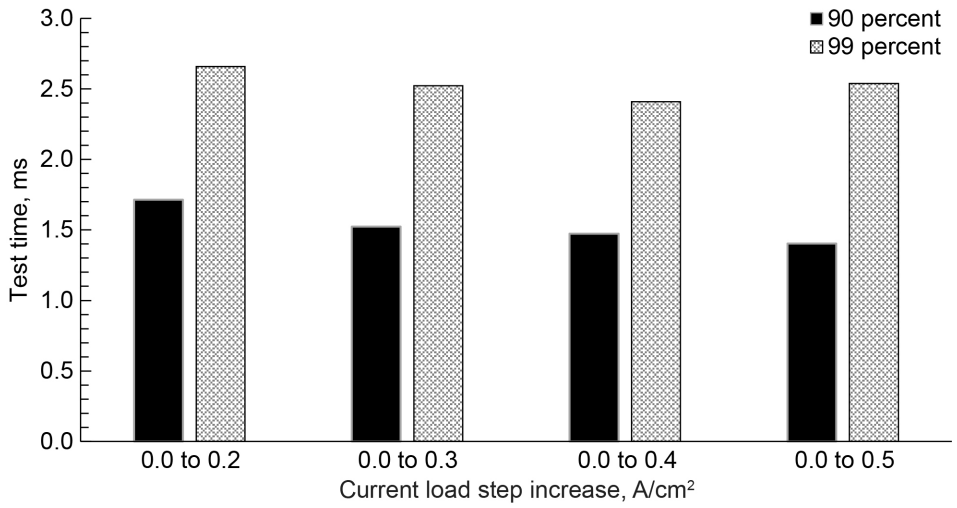

Figure 8.—Times to average fuel cell voltage at 90 and 99 percent of final change following current load step increases.

If the values recorded at 30 s after the current step are not the true steady state or the utilized level of data smoothing is inadequate for a particular case, the determined times could be altered significantly.

Step Decrease

Figure 9 shows the average cell potential and current density results for the current load step decreases.

Figure 10 shows the times for current load to reach 90 and 99 percent of the final current density change, comparing the final steady-state current density and initial current density for the cases of current load decrease. The times to achieve 90 percent of the current change for a step decrease are ~1/10 the time required for a step increase. Additionally, larger current step decreases required less time to approach the final steady-state value.

Faster response is known to occur during decreasing load cases, potentially because of improved GDL mass transport and membrane hydration achieved at the prior steady-state higher current density operation (Ref. 7). Gas diffusion through GDL is on the order of 10 ms (Refs. 7 and 8), which may be too long to influence the results presented here. Decreasing current steps that result in high final cell voltages can result in a reversal of the cell current that leads to fuel cell electrode damage (Ref. 6), though no evidence of such current reversal or performance impairment was found for the NFT stack studied here.

Figure 11 displays the times for average cell voltage to reach 90 and 99 percent of the final voltage change between initial and final steady-state values for current load step decreases. The voltage response took longer in all cases for the current load step decrease compared to the corresponding step increase case. Although less time was needed for average cell voltage to reach 90 percent of the final value for larger current load changes, all cases except 0.2 to 0 A/cm^2 took ~3.6 ms to get to 99 percent of the final value, almost a full millisecond longer than the current load increase cases.

It has previously been noted that fuel cells respond slower for steps with higher final steady-state voltages (Ref. 6). This was attributed to the cathode charge transfer process. Thus, a step from high cell voltage to low cell voltage (i.e., increasing current step) should take less time than the return step back to high cell voltage (i.e., decreasing current step).

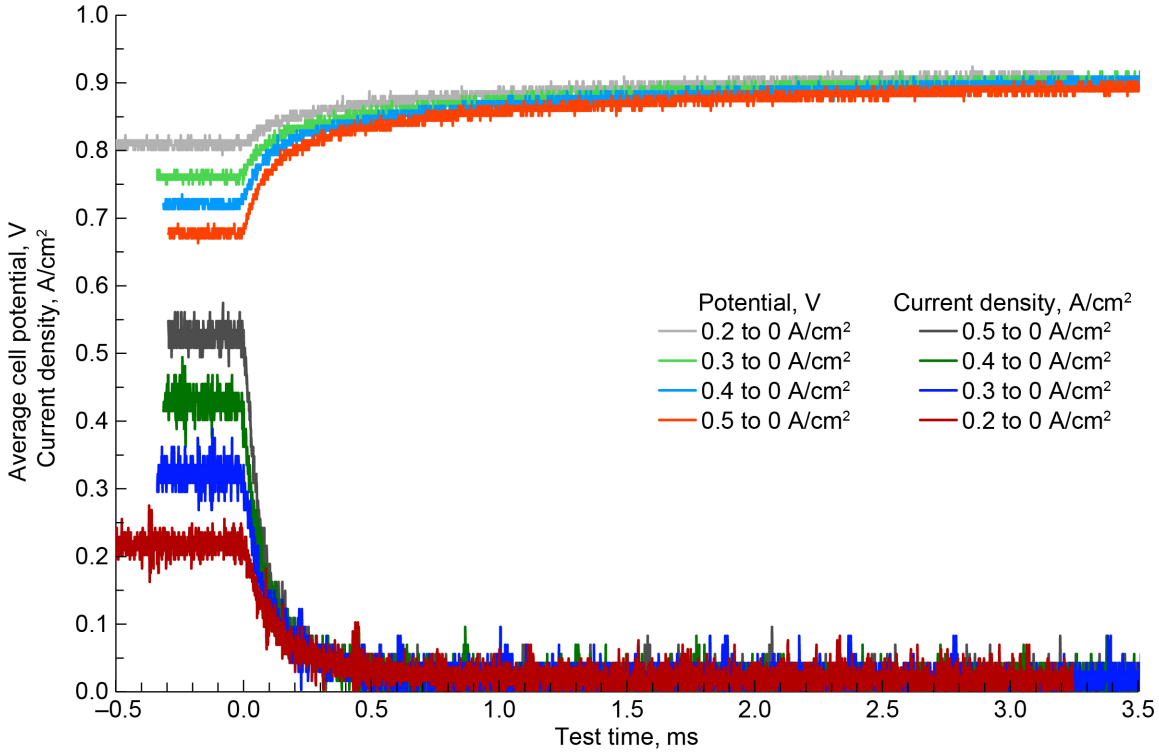

Figure 9.—Average fuel cell potential and current density for current load step decreases where test time 0 ms indicates load change command.

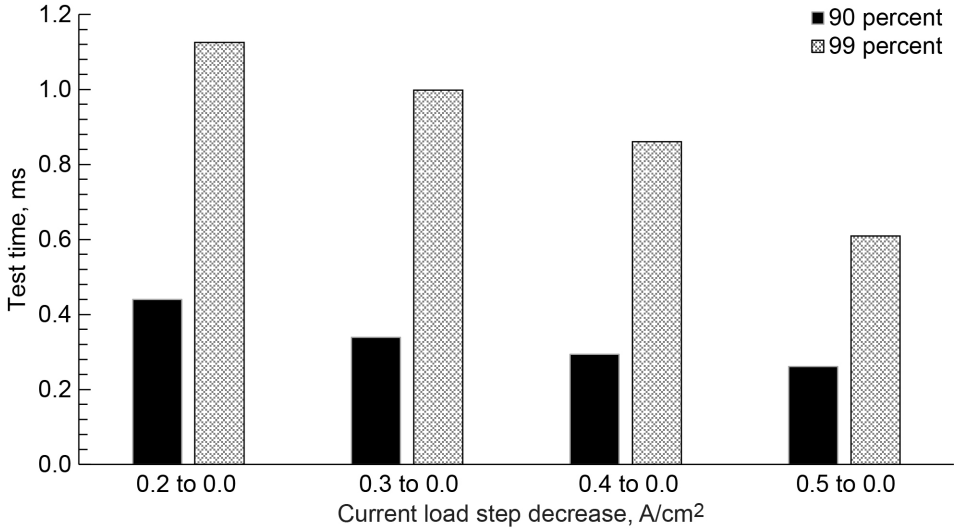

Figure 10.—Times to fuel cell current load at 90 and 99 percent of final change following current load step decreases.

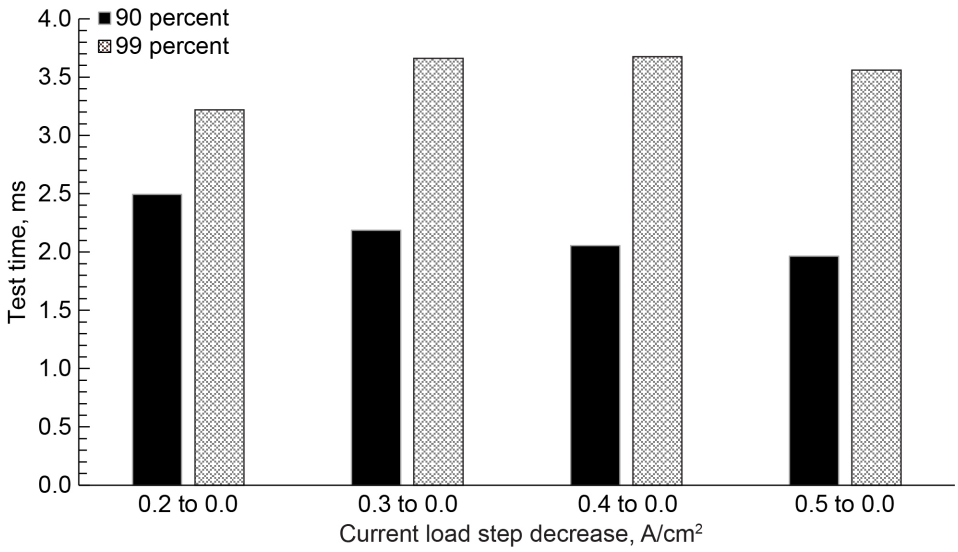

Figure 11.—Times to average fuel cell voltage at 90 and 99 percent of final change following current load step decreases.

Increasing Power Pulse Case

One additional case was performed where current load was held steady at a current density of 0.1 A/cm^2, stepped up to 0.5 A/cm^2 for 45 ms, and then returned to 0.1 A/cm^2 as shown in Figure 12. As a result of the longer timescale of this case, the same 0.8-μs data sampling rate was not possible for this case, and voltage undershoot and overshoot are not discernable here. Slight current load overshoot representing the inrush current is visible just after test time 0 ms, and current load undershoot is apparent leading up to 50 ms. The stack appears to reach new steady-state conditions after several milliseconds for each change.

Batteries are perhaps the most critical comparison for fuel cell transient load operation and high-power pulses, in particular. Batteries are used for power in many relevant applications including railguns, which require high-power pulsed operation (Ref. 10). Batteries have been demonstrated to support significant loads (5,000 A) lasting 0.5 to 15 ms, although the times to steady state appeared to be greater than 15 ms (Ref. 9). Current overshoot behavior only occurred with load increases in the present study, producing peak currents as much as 20 percent greater than steady-state values. No voltage undershoot behavior was observed with the studied batteries.

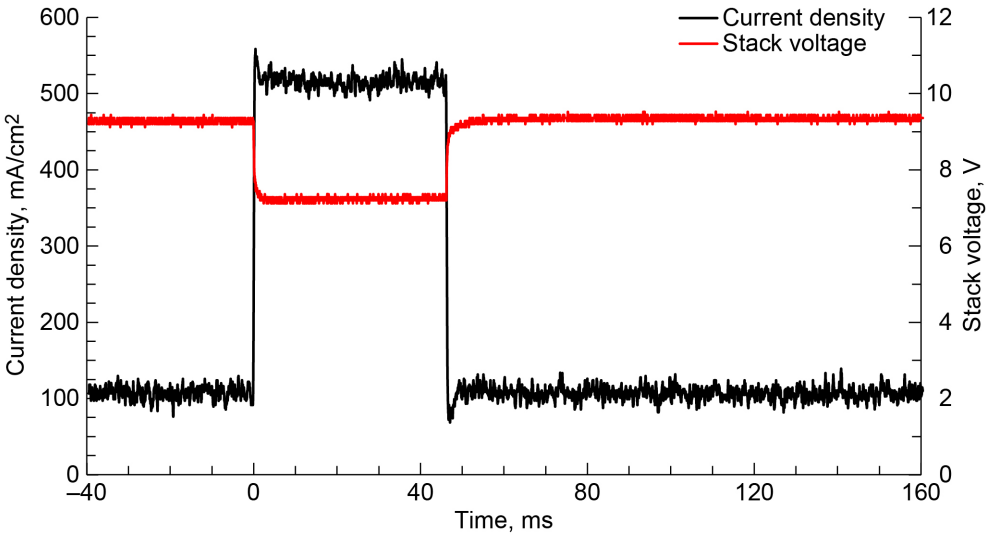

Figure 12.—Fuel cell stack voltage response to stepping current density from 0.1 to 0.5 and back to 0.1 A/cm^2.

Conclusions

Many spaceflight mission power profiles require the power system to support all changes in load, in addition to being energy dense. H_2-O_2 proton exchange membrane (PEM) fuel cells can accommodate such requirements without significant current smoothing or additional devices such as capacitors or batteries to provide transient power. These experiments characterized PEM fuel cell stack response to increasing and decreasing load step changes up to 0.5 A/cm^2, thereby meeting one of the major goals of expected future mission load profiles. In all cases, the fuel cell output voltage stabilized within 4 ms of a load step change. No noticeable performance degradation occurred when the fuel cell was exposed to transient overshoot current density loads of up to ~1.5 A/cm^2 as imposed on the stack by an external load control system.

Faster response generally occurred during decreasing load cases and for larger current step changes, though it is difficult to separate electrochemical effects from the influence of slew rate limitation provided by the chosen hardware. Preferred follow-on experimental setups would utilize rapid switching between resistors rather than an electronic load to minimize external to the fuel cell stack effects on the measured response.

Appendix—Raw Data

The unsmoothed current sensor output voltage and the 12-cell proton exchange membrane (PEM) fuel cell stack voltage data for all current load step change cases is provided in Figure 13 to Figure 21.

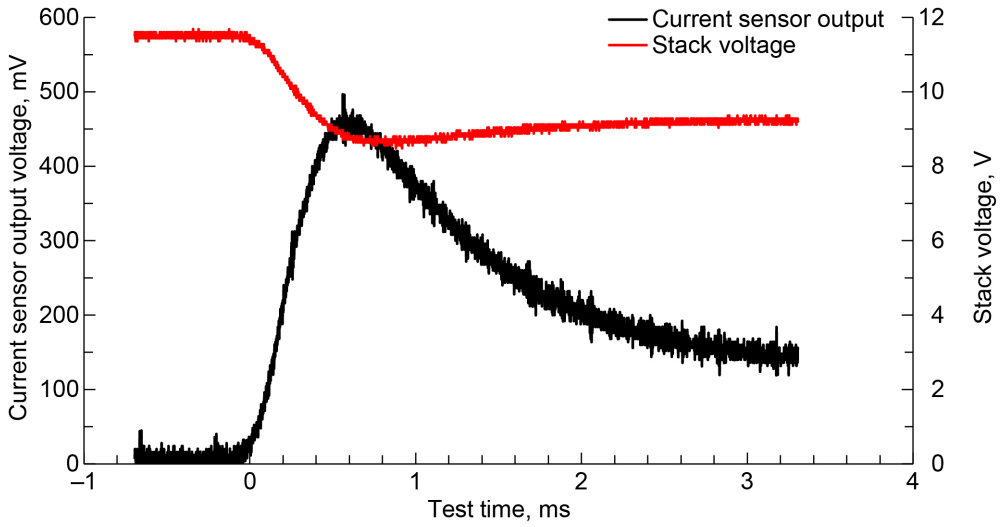

Figure 13.—0.0 to 0.2 A/cm^2.

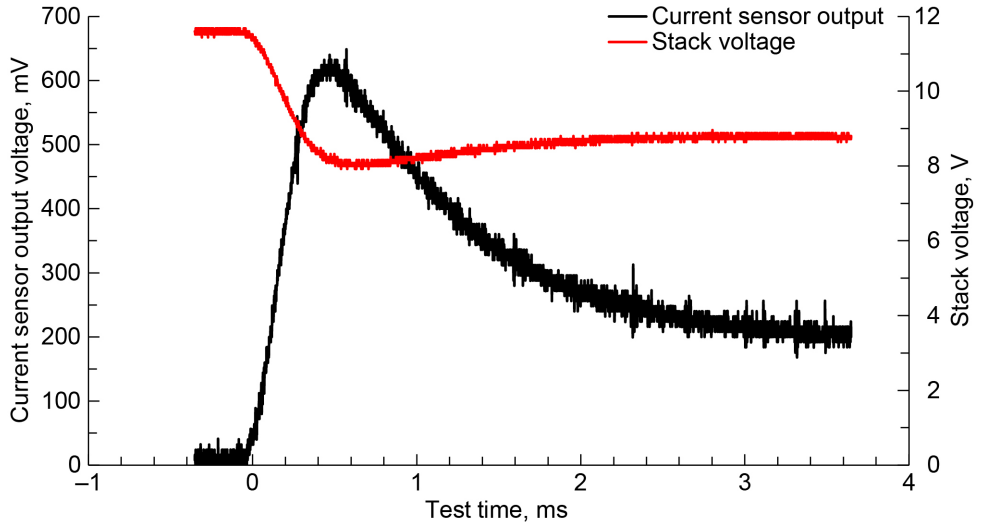

Figure 14.—0.0 to 0.3 A/cm^2.

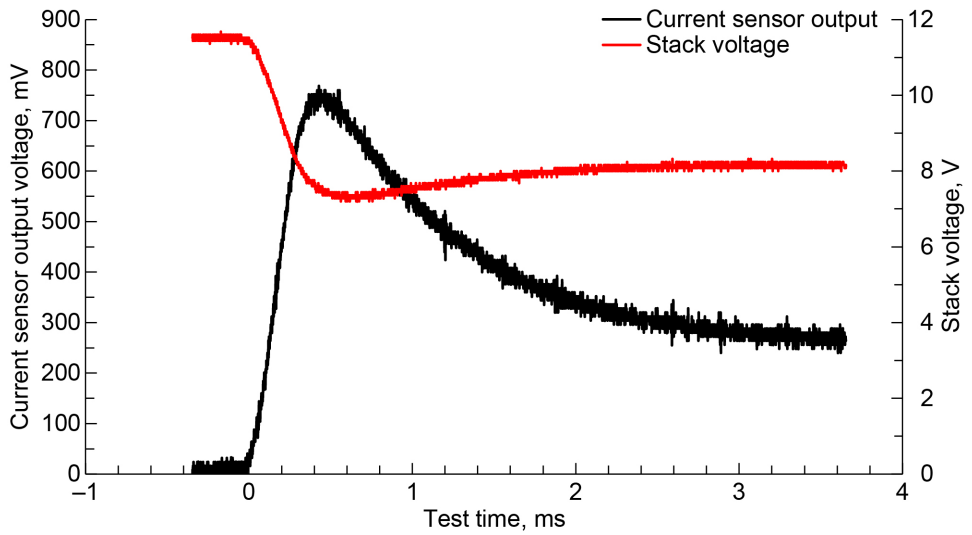

Figure 15.—0.0 to 0.4 A/cm^2.

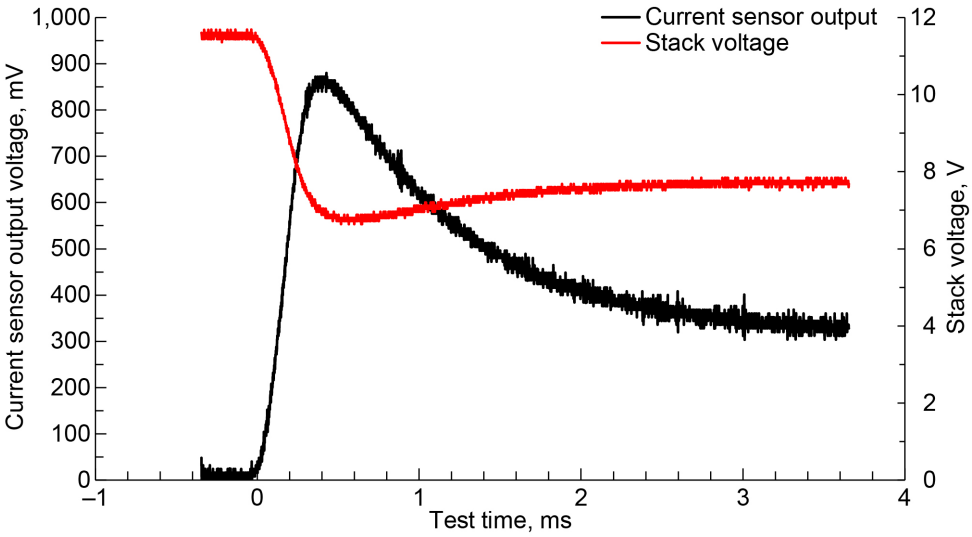

Figure 16.—0.0 to 0.5 A/cm^2.

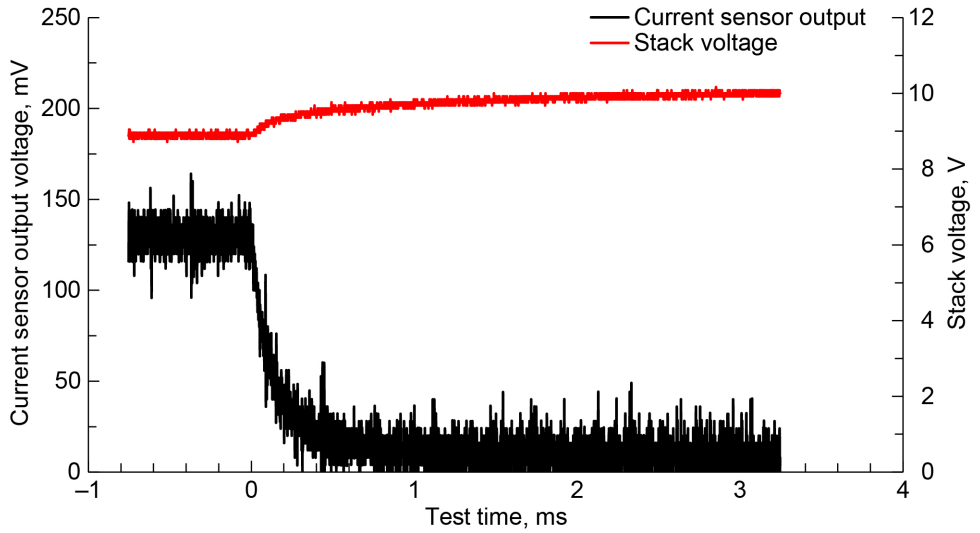

Figure 17.—0.2 to 0.0 A/cm^2.

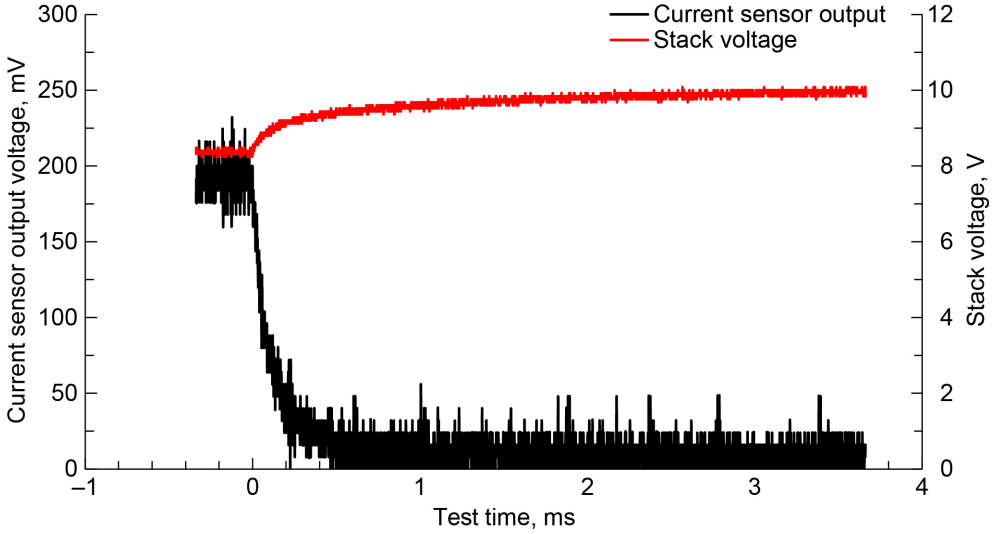

Figure 18.—0.3 to 0.0 A/cm^2.

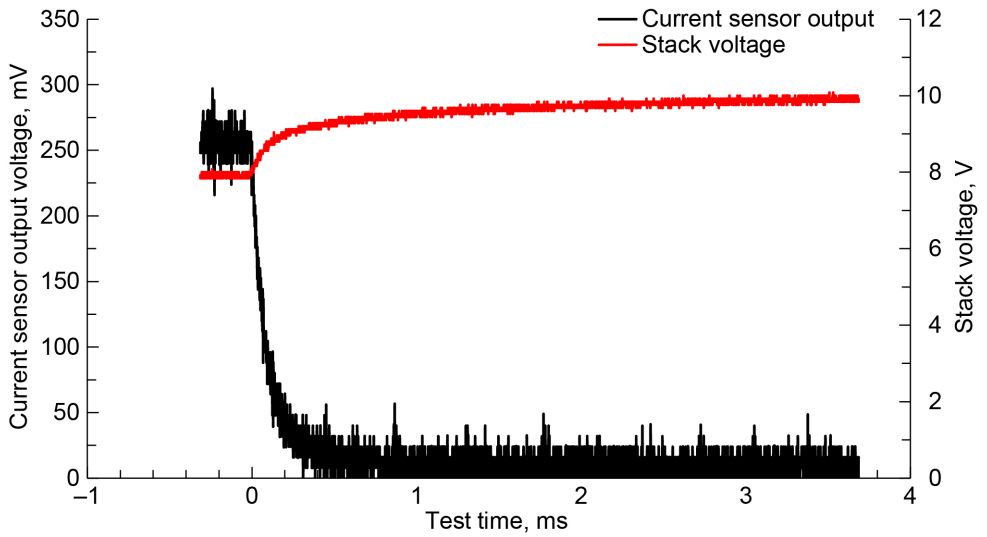

Figure 19.—0.4 to 0.0 A/cm^2.

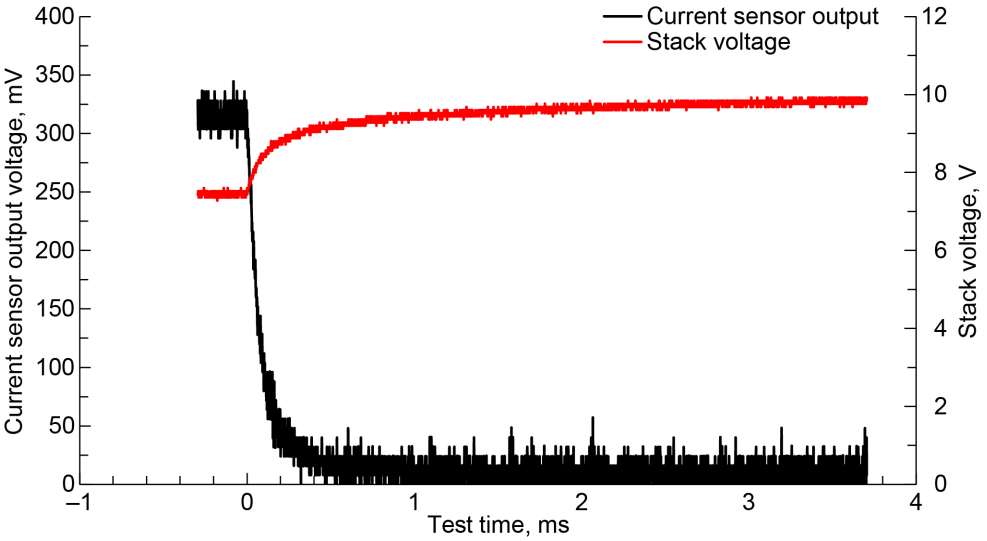

Figure 20.—0.5 to 0.0 A/cm^2.

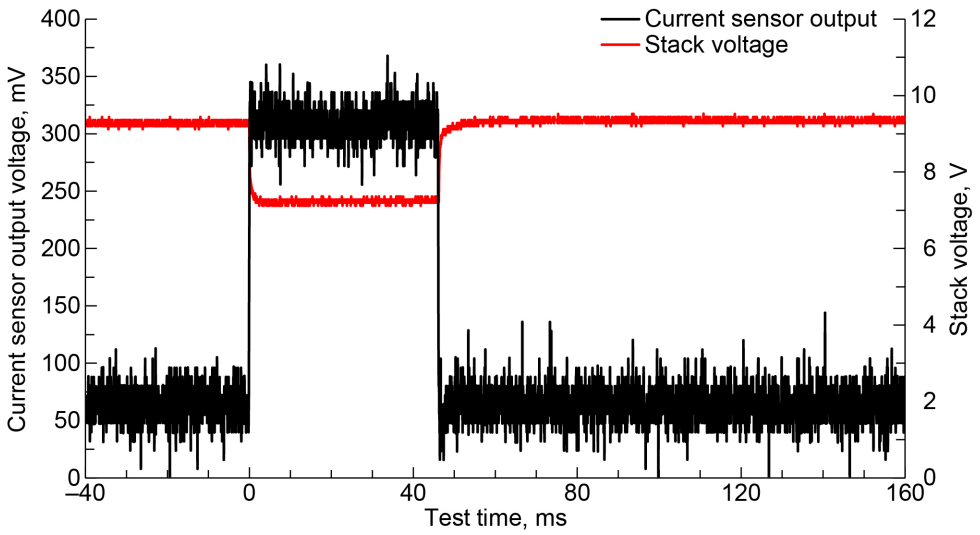

Figure 21.—0.1 to 0.5 to 0.1 A/cm^2.

References

1. Hou, Yongping; Yang, Zhihua; and Wan, Gang: An Improved Dynamic Voltage Model of PEM Fuel Cell Stack. Int. J. Hydrog. Energy, vol. 35, no. 20, 2010, pp. 11154–11160.
2. Gilligan, Ryan P., et al.: Structural Dynamic Testing Results for Air-Independent Proton Exchange Membrane (PEM) Fuel Cell Technologies for Space Applications. IMECE2019–11691, 2019.
3. Smith, Phillip J., et al.: Effect of Reactant Purity on Proton Exchange Membrane Fuel Cell Performance. NASA/TP-20205011711, 2021. https://ntrs.nasa.gov
4. Smith, Phillip J., et al.: Effect of Reactant Pressure on Proton Exchange Membrane Fuel Cell Performance. NASA/TP-20205011192, 2021. https://ntrs.nasa.gov
5. Sunhoe Kim; Shimpalee, S.; and Van Zee, J.W.: Effect of Flow Field Design and Voltage Change Range on the Dynamic Behavior of PEMFs. J. Electrochem. Soc., vol. 152, no. 6, 2005, pp. A1265–A1271.
6. Weydahl, Helge, et al.: Transient Response of a Proton Exchange Membrane Fuel Cell. J. Power Sources, vol. 171, no. 2, 2007, pp. 321–330.
7. Cho, Junhyun; Kim, Han-Sang; and Min, Kyoungdoug: Transient Response of a Unit Proton-Exchange Membrane Fuel Cell Under Various Operating Conditions. J. Power Sources, vol. 185, no. 1, 2008, pp. 118–128.
8. Edwards, Russell L.; and Demuren, Ayodeji: Regression Analysis of PEM Fuel Cell Transient Response. Int. J. Energy Environ. Eng., vol. 7, 2016, pp. 329–341.
9. Chen, Y. Yvonne; and Sitzman, Alex: Testing a Lithium Ion Battery as a Pulse Power Source. Proceedings of the 2005 IEEE Pulsed Power Conference, 2005, pp. 485–488.
10. O'Shea, Paul: U.S. Navy Powers Railgun With Batteries. Electron. Prod., 2016. https://www.electronicproducts.com/u-s-navy-powers-railgun-with-batteries/# Accessed Oct. 6, 2021.